Monopoles in Maximal Abelian gauge, number of zero modes, and instantons

Adriano Di Giacomo

University of Pisa, Department of Physics and INFN, Sezione di Pisa, Largo B. Pontecorvo 3, 56127, Pisa, Italy

Masayasu Hasegawa

Joint Institute for Nuclear Research, Bogoliubov Laboratory of Theoretical Physics, Dubna, 141980, Moscow, Russia

(Dated: April 28, 2015)

Abstract

In this short contribution we report relations between the Abelian monopoles in the Maximal Abelian gauge, the number of zero modes of Overlap femions, and instantons. We show that the number of zero modes increase with the total physical length of monopole loops. The number of instantons is directly proportional to the total physical length of monopole loops. These features support the results in Ref. [1].

1 Introduction

We study the relations between chiral symmetry breaking, instantons, and monopoles using the computers at the Cybermedia Center and Research Center for Nuclear Physics (University of Osaka), and at the Yukawa Institute for Theoretical Physics (University of Kyoto). In order to investigate the relations, we use Overlap fermions which hold the chiral symmetry in the lattice gauge theory as a tool [2, 3, 4, 5, 6, 7, 8, 9, 10, 11]. We have reported our research results as follows [1, 12]:

First, we generate SU(3) quenched configurations. We construct the Overlap Dirac operator from the gauge links, and solve the eigenvalue problems. We then count the zero modes in the spectra of the Overlap Dirac operator as the number of instantons. However, we never observed zero modes of plus and minus chiralities in the same configuration. We always observe the zero modes which are only plus **or** minus chiralities in the same configuration; topological charges. Therefore, we find that the number of instantons N_I is counted from the values of the average square of the topological charges $\langle Q^2 \rangle$. We show that the instanton density is consistent with the result of the instanton liquid model [13].

Next, we generate SU(3) quenched configurations adding one pair of monopoles with charges $m_c = 0, 1, 2, 3, 4$ by the monopole creation operator [14]. We confirm that the additional monopoles make only the long monopole loops, and the length of the monopole loops increases with the monopole charges. Moreover, the number of zero modes, and the number of instantons increase with the monopole charges. Then, we show that one magnetic charge $m_c = 1$ makes one (+ or -) instanton by comparing with our predictions.

Moreover, we compute the chiral condensate that is an order parameter of chiral symmetry breaking from low-lying eigenvalues and eigenvectors of the Overlap Dirac operator. We show that the additional monopoles induce chiral symmetry breaking.

In this study, first, we diagonalize normal SU(3) quenched configurations by the Maximal Abelian gauge (MAG), and calculate the monopole currents from Abelian link variables after the Abelian projection. The monopole currents make loops because of the conservation law, there-

This report is a contribution to the HPC journal.

fore, we measure the total length of monopole loops and evaluate the monopole density [15, 16, 17, 18, 19, 20]. We find that the numbers of zero modes, and the number of instantons increase with the total physical length of monopole loops. These features support the above results [1]. Moreover, the number of instantons is directly proportional to the total physical length of monopole loops.

The contents of this contribution are as follows: First, we shortly review our research. Second, we briefly introduce Abelian monopoles. Last, we evaluate quantitatively the physical length of Abelian monopole loops, the number of zero modes, and instantons.

2 Overlap fermions

We use Overlap fermions which hold the chiral symmetry in the lattice gauge theory [2, 3]. In our study, first, we generate SU(3) quenched configurations, and compute the Wilson Dirac operator $D_W(\rho) = D_W - \frac{\rho}{a}$ from the gauge links. The mass less Wilson Dirac operator is D_W. The (negative) mass parameter is used $\rho = 1.4$ in our simulation. The lattice spacing is a. Then, we compute the sign function $\varepsilon(H_W(\rho))$ of the Hermitian Wilson Dirac operator $H_W(\rho) = \gamma_5 D_W(\rho)$ as follows:

$$\varepsilon(H_W(\rho)) \equiv \frac{H_W(\rho)}{\sqrt{H_W(\rho)^\dagger H_W(\rho)}}. \quad (1)$$

Last, the Overlap Dirac operator is defined by the sign function as follows:

$$D(\rho) = \frac{\rho}{a}\{1 + \gamma_5 \varepsilon(H_W(\rho))\} \quad (2)$$

These operations have already been carried out by other groups [5, 7, 9, 8, 11].

The eighty pairs of low-lying eigenvalues and eigenvectors are computed from one configuration using the subroutines of ARPACK. Most of the computation time is spent to solve the eigenvalue problems of the Overlap Dirac operator.

Our computer programs are vectorized and parallelized for the supercomputers (SX-8, SX-9, SX-ACE). For example, the vectorization rate is 99.8% using four cores in one node (SX-ACE). The computation time by use of SX-ACE is compared the Wilson Dirac operator with the Overlap Dirac operator each the number of zero modes N_{Zero} in Table 1.

Table 1: The computation time (user time in hour unit) of the Wilson (W) and Overlap (Ov) Dirac operators. One configuration is used each measurement. β = 6.00. SX-ACE is used.

OP	V	$N_Z = 0$	$N_Z = 1$	$N_Z = 2$	$N_Z = 3$
W	$14^3 28$	0.9	0.9	0.9	1.0
	18^4	1.3	1.2	1.2	1.6
	$16^3 32$	1.5	1.6	1.7	1.8
Ov	$14^3 28$	7.7	7.7	8.4	9.2
	18^4	12.2	16.9	14.0	14.3
	$16^3 32$	23.1	24.0	26.7	22.5

2.1 Zero modes, the topological charge, and the topological susceptibility

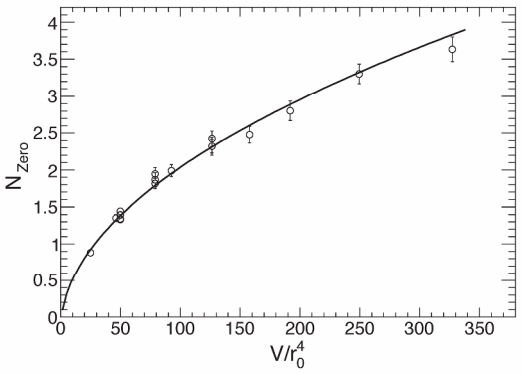

Figure 1: The number of zero modes N_{Zero} vs the physical volume V/r_0^4. The figure is been updated (Fig. 3 in Ref. [1]).

The zero modes of plus chiralities are defined as n_+, and minus chiralities are defined as n_-. The observed number of zero modes N_{Zero} in our simulations is averaged by the number of configurations, and increases with physical volume as shown in Fig. 1. The function $N_{Zero} = \sqrt{A \cdot V/r_0^4} + B$ is fitted. The fitting results are $A = 4.9(3) \times 10^{-2}$, $B = -0.19(5)$, $\chi^2/d.o.f = 15.3/16.0$.

The topological charges Q is defined as $Q = n_+ - n-$. In our simulations there is one relation; $N_{Zero} = |Q|$. The average square of topological charges $\langle Q^2 \rangle$ with the physical volume is shown in Fig. 2. The function $\langle Q^2 \rangle = A \cdot V/r_0^4 + B$

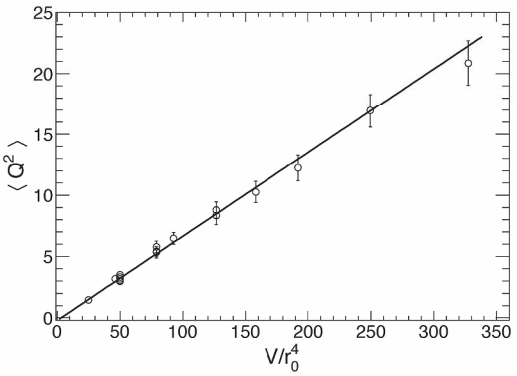

Figure 2: The average square of topological charges $\langle Q^2 \rangle$; the number of instantons N_I vs the physical volume V/r_0^4. The figure is been updated (Fig. 4 in Ref. [1]).

is fitted. The fitting results are $A = 6.9(2) \times 10^{-2}$, $B = -0.2(0.12)$, $\chi^2/d.o.f = 12.4/16.0$.

The topological susceptibility is computed from the average square of topological charges $\langle Q^2 \rangle$ divided by physical volume V/r_0^4. We use from 200 to 895 configurations each measurement. The lattice spacing in our simulations is computed from the analytic function in Ref. [21]. The Sommer scale is $r_0 = 0.5$ [fm]. We list our results together with simulation parameters in Table II of Ref. [1]. In this contribution, we add new results of $V = 14^3 \times 28$, $\beta = 6.00$, $N_{conf} = 400$.

The topological susceptibility in the continuum limit is obtained by fitting a function $\langle Q^2 \rangle r_0^4/V = A + B(a/r_0)^2$ as in Ref. [7]. We fix the physical volume $V/r_0^4 = 49.96$, and extrapolate the topological susceptibility in the continuum limit from the five data points. Our result of the topological susceptibility is

$$\chi = (1.86(6) \times 10^2 \text{ [MeV]})^4. \quad (3)$$

This result is consistent with the numerical simulations of Ref. [8] and Ref. [9]. Moreover, these results are consistent with the theoretical expectation [22, 23]. Therefore, the computations of Overlap Dirac operator are appropriately carried out.

2.2 Instantons

We want to count the number of instantons N_I from the number of zero modes ($n_+ + n_-$), because there is the Atiyah-Singer index theorem [24]. However, we never observed the zero modes of the plus chiralities n_+ and minus chiralities n_- from the same configuration at the same time. The observed zero modes are **net** numbers of the zero modes $n_+ - n_-$ (topological charges). Therefore, we compute the number of zero modes ($n_+ + n_-$) by analytical computations, and we find that the number of instantons is obtained as the average square of the topological charges ($N_I = \langle Q^2 \rangle$). We compute the instanton density ρ_i by fitting a linear function to the results of the average square of topological charges $\langle Q^2 \rangle$ as shown in Fig. 2. The instanton density is

$$\rho_i = 8.3(3) \times 10^{-4} \text{ [GeV}^4\text{]}. \quad (4)$$

This result is consistent with the result of the instanton liquid model [13].

2.3 Abelian monopoles in MAG

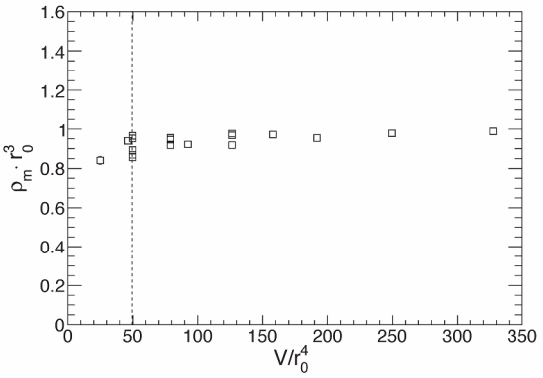

Figure 3: The monopole density $\rho_m \cdot r_0^3$ vs the physical volume V/r_0^4. The dotted line indicates $V/r_0^4 = 49.96$.

We perform the computations as in Ref. [20]. First, we iteratively diagonalize the non-Abelian link variables in Maximal Abelian Gauge (MAG) using the Simulated Annealing algorithm in order to prevent the effects on Gribov copies. The number of iterations is 20. Then we extract Abelian link variables holding the $U(1) \times U(1)$ symmetry by the Abelian projection from the non-Abelian link variables. Next, we define the monopole currents $k_\mu^i(n)$ as in Ref. [18, 19].

The monopole currents obey the conservation law $\sum_i k_\mu^i(n) = 0$. Therefore, the monopole currents form loops.

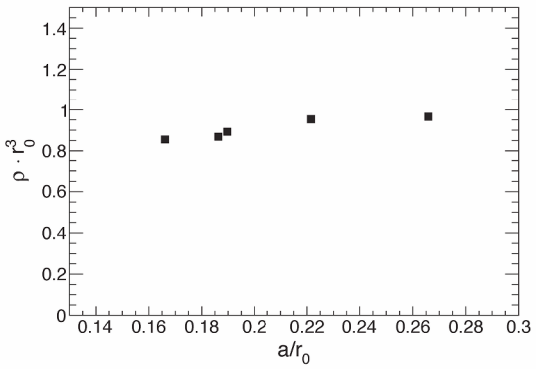

Figure 4: The monopole density in the continuum limit. The physical volume is $V/r_0^4 = 49.96$, and five results of β = 5.81, 5.90, 5.99, 6.00, 6.07 are used.

The physical monopole density is computed by summing all of the indexes of monopole currents as follows [20]:

$$\rho_m r_0^3 = \frac{1}{12V} \sum_i \sum_{n,\mu} |k_\mu^i(n)| r_0^3. \tag{5}$$

In this study we define the total physical length of monopole loops as follows:

$$l_m/r_0 \equiv \frac{1}{12} \sum_i \sum_{n,\mu} |k_\mu^i(n)|/r_0. \tag{6}$$

This definition is different from Ref. [17] in order to evaluate the monopole density by fitting a function. The simulation parameters of the lattices (β and V) are the exactly same as the previous section 2.1.

The values of the monopole density and the length of monopole loops are the dependent on the choice of the gauges. However, several studies in quenched SU(2) without fixing the gauges are done [25, 26].

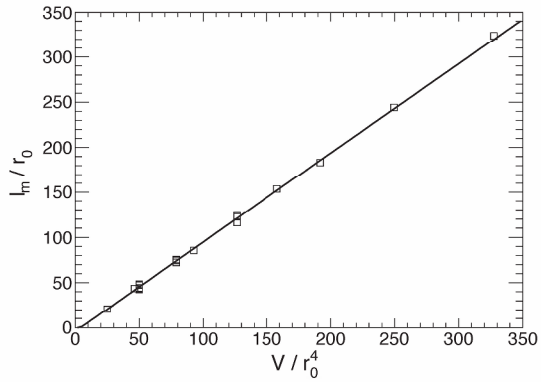

Figure 5: The total physical length of monopole loops l_m/r_0 vs the physical volume V/r_0^4.

First, we check effects of the monopole density on the physical volume as shown in Fig. 3. The results does not have large finite volume effects. Next, we check the monopole density in the continuum limit from five data points of $V/r_0^4 = 49.96$ as shown in Fig. 4.

The total physical length of monopole loops is in direct proportion to the physical volume as shown in Fig. 5. The function $l_m/r_0 = A \cdot V/r_0^4 + B$ is fitted. The fitting results are $A = 0.989(4)$, $B = -4.0(3)$, and $\chi^2/d.o.f. = 140.3/16.0$. The value of $\chi^2/d.o.f.$ is large, because the errors of the data are too small. We evaluate the monopole density by the same way as the instanton density. The proportion A becomes the monopole density $\rho_m \cdot r_0^3$, and the value is consistent with Ref. [20]. We evaluate the monopole density as

$$\rho_m = 6.08(2) \times 10^{-2}\ [\mathrm{GeV}^3]. \tag{7}$$

2.4 Abelian monopoles, number of zero modes, and instantons

Lastly, we check the relations between the Abelian monopoles, the number of zero modes, and instantons. We quantitatively evaluate the relations by fitting the same functions as in Fig. 1, and Fig. 2.

The number of zero modes N_{Zero} increases with the square root of the total physical length of monopole loops l_m/r_0 as shown in Fig. 6. The function $N_{Zero} = \sqrt{A \cdot l_m/r_0} + B$ is fitted. The fitting results are $A = 4.7(3) \times 10^{-2}$, $B = -8(5) \times 10^{-2}$, and $\chi^2/d.o.f. = 10.7/16.0$. This behavior is the same as Fig. 1.

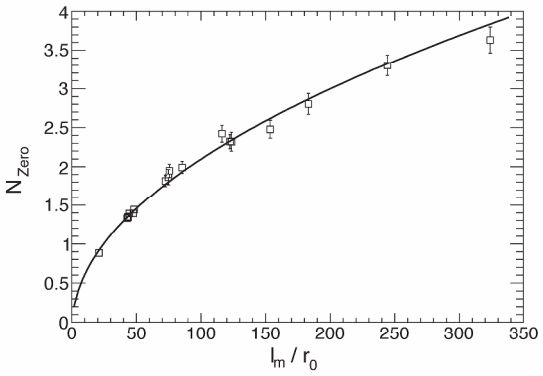

Figure 6: The zero modes N_{Zero} vs the total physical length of monopole loops l_m/r_0.

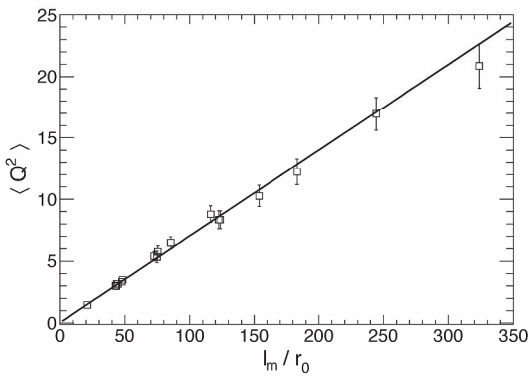

Figure 7: The number of instantons N_I ($\langle Q^2 \rangle$) vs the total physical length of monopole loops l_m/r_0.

The number of instantons N_I increases with the total physical length of monopole loops l_m/r_0 as shown in Fig. 7. The function $\langle Q^2 \rangle = A \cdot l_m/r_0 + B$ is fitted. The fitting results are $A = 7.0(2) \times 10^{-2}$, $B = 0.05(0.12)$, and $\chi^2/d.o.f. = 6.4/16.0$. The intercept B = 0, and $\chi^2/d.o.f. = 6.4/16.0$, therefore, the number of instantons is in direct proportion to the total physical length of monopole loops.

3 Summary and conclusions

First, we briefly review our study. Next, we use SU(3) quenched configurations that are diagonalized in Maximal Abelian gauge, and compute the monopole density and the total physical length of monopole loops from Abelian link variables.

The total physical length of monopole loops is directly proportional to the physical volume. The number of zero modes increases with the square root of the total physical length of monopole loops. The number of instantons is in direct proportion to the total physical length of monopole loops.

Incidentally, we have reported the results that the number of zero modes, and the number of instantons increase with the length of monopole loops increasing [1].

The results in this contribution support this feature.

4 Acknowledgments

We really appreciate the computer resources and technical supports by the Research Center for Nuclear Physics and the Cybermedia Center at the University of Osaka. And also, we use SR16000 at the Yukawa Institute for Theoretical Physics at the University of Kyoto.

References

[1] A. Di Giacomo, and M. Hasegawa, Phys. Rev. **D 91** (2015) 054512.

[2] P. H. Ginsparg, and K. G. Wilson Phys. Rev. D **25** (1982) 2649.

[3] N. Neuberger, Phys. Lett. B **427** (1998) 353.

[4] S. Capitani, C. Göckeler, R. Horsley, P. E. L. Rakow, and G. Schierholz, Phys. Lett. B **468** (1999) 150.

[5] R. G. Edwards, U. M. Heller, J. Kiskis, R. Narayanan, Phys. Rev. D **61** (2000) 074504.

[6] L. Giusti, C. Hoelbling, M. Lüscher, and H. Wittig, Comput. Phys. Commun. **153** (2003) 31.

[7] L. Giusti, M. Lüscher, P. Weisz, and H. Wittig, J. High Energy Phys. **11** (2003) 023.

[8] L. Del Debbio, and C. Pica, J. High Energy Phys. **02** (2004) 003.

[9] L. Del Debbio, L. Giusti, and C. Pica, Phys. Rev. Lett. **94** (2005) 032003.

[10] D. Galletly, M. Gurtler, R. Horsley, H. Perlt, P. E. L. Rakow, G. Schierholz, A. Schiller, and T. Streuer, Phys. Rev. D **75** (2007) 073015.

[11] E.-M. Ilgenfritz, K. Koller, Y. Koma, G. Schierholz, T. Streuer, and V. Weinberg, Phys. Rev. D **76** (2007) 034506.

[12] A. Di Giacomo, and M. Hasegawa, arXiv: 1412.2704.

[13] E. V. Shuryak, Nucl. Phys. **B203** (1982) 93; Nucl. Phys. **B203** (1982) 116; Nucl. Phys. **B203** (1982) 140.

[14] C. Bonati, G. Cossu, M. D'Elia, and A. Di Giacomo, Phys. Rev. D **85** (2012) 065001.

[15] G. 't Hooft, Nucl. Phys. **B190** (1981) 455.

[16] T. A. DeGrand, and D. Toussaint, Phys. Rev. D **22** (1980) 2478.

[17] A. S. Kronfeld, G. Schierholz, and U.-J. Wiese, Nucl. Phys. B **293** (1987) 461.

[18] F. Brandstaeter, G. Schierholz, and U.-J. Wiese, Phys. Lett. B **272** (1991) 319.

[19] M. I. Polikarpov, and K. Yee, Phys. Lett. B **316** (1993) 333.

[20] V. G. Bornyakov, H. Ichie, Y. Koma, Y. Mori, Y. Nakamura, D. Pleiter, M. I. Polikarpov, G. Schierholz, T. Streuer, H. Stüben, and T. Suzuki, and DIK collaboration, Phys. Rev. D **70** (2004) 074511.

[21] S. Necco, and R. Sommer Nucl.Phys. **B622** (2002) 328.

[22] G. Veneziano, Nucl. Phys. **B159** (1979) 213.

[23] E. Witten, Nucl. Phys. **B156** (1979) 269.

[24] M. F. Atiyah, and I. M. Singer, Bull. Amer. Math. Soc. 69 (1963), 422-433.

[25] T. Suzuki, K. Ishiguro, Y. Koma, and S. Toru, Phys. Rev. **D 77** (2008) 034502.

[26] T. Suzuki, M. Hasegawa, K. Ishiguro, Y. Koma, and S. Toru, Phys. Rev. **D 80** (2009) 054504.